Acoust. Sci. & Tech. **41**, 5 (2020)

PAPER

Effect of horizontal sound-absorptive strips inside closed rooms

Takumi Asakura[1,*], Wataru Yashima[1] and Fumiaki Satoh[2]

[1]*Tokyo University of Science,*
2641, Yamazaki, Noda, 278–0022 Japan
[2]*Chiba Institute of Technology,*
2–17–1, Tsudanuma, Narashino, 275–0016 Japan

(*Received 2 July 2019, Accepted for publication 7 January 2020*)

Abstract: The sound absorption characteristics obtained with horizontally arranged sound-absorptive strips on walls were evaluated by objective measure based on the acoustical indices determined from the impulse responses calculated by finite-difference time-domain simulation. The subjective effect of the horizontal sound-absorptive strips (HSSs) was also investigated by subjective measure based on Scheffe's paired comparison method. The results of the numerical case study confirmed that the frequency characteristics of the acoustic indices of rooms with the HSSs significantly changed under the influence of the relative positional relationship between the source and receiving points and the arrangement height of the strips. Through a subjective evaluation experiment, the differences in the absorption effect of various types of settings of the strips on the reverberation inside rooms were also clarified.

Keywords: Sound-absorptive strip, Finite-difference time-domain method, Room-acoustic indices, Scheffe's paired comparison method

PACS number: 43.55.+p [doi:10.1250/ast.41.709]

1. INTRODUCTION

Appropriate absorption treatment inside habitable spaces considerably contributes to the improvement of the sound environment. Providing sufficient absorption materials to wide areas on the surfaces of walls or ceilings leads to the sufficient suppression of reverberation in rooms; however, it is desirable that the total area of absorbers is kept minimum from the viewpoint of reduction of installation cost, design, and functionality. Parvanian and Panjepour [1] indicated that the optimization of the sound absorbing characteristics of porous materials under limited dimensions of the absorber is important. In a practical case such as construction works, to maximally improve the efficiency of the arrangement of absorption, the placement of absorbent materials in patches is a relatively common situation. For such a reason, the maximization scheme of the efficiency of absorption by using a limited amount of absorption materials is of considerable importance.

The sound absorption characteristics of absorptive strips periodically attached on walls have been focused as an important issue in the field of acoustics. There have been some classical studies [2–7] on the basic issues of absorptive materials periodically set in a strip structure. Chrisler indicated that measurements on small material samples lead to larger absorption results than predicted by theory [2]. In relation to that, when the absorption materials are placed in patches, the absorption may be overestimated [3], and this has been generally attributed to the edge effect. Takahashi has investigated the effect of excess sound absorption due to the periodic arrangement of absorptive materials [6]. Guicking has also investigated the excess absorption effect of an infinite absorbing strip [7]. In recent studies, the sound absorption of periodic absorptive devices has also been investigated [8–13]. Ducourneau and Planeau [8] generalized the numerical method of determination of an equivalent acoustic absorption model of flat heterogeneous walls presented in industrial rooms. Park *et al.* discussed the acoustic effect of periodically arranged sound-absorptive strips on the interior sound fields inside rooms using the mean acoustic potential energy density distribution [9]. From a similar viewpoint of application study, by using experimental and numerical schemes, Yasuda *et al.* studied the reverberation characteristics caused by unevenly distributed absorbers [13]. While many of these studies focus on the basic physical characteristics of periodically arranged absorptive materials, there are

*e-mail: t_asakura@rs.tus.ac.jp

a few that focused on more detailed performances of partially and unevenly arranged absorbers under more specific room conditions. Although basic findings are of considerable importance to apply absorptive materials to practical cases, the sound absorption characteristics of absorbers can also be greatly affected by, for example, the dimensions of the rooms and the spatial relationships among the source, receiver, and absorber.

In this study, the acoustical effect of the HSS treatment of surrounding walls inside two types of small rooms of specific dimensions is investigated through a numerical study based on the wave-based method of the finite-difference time-domain (FDTD) method. Considering such general spaces as small meeting rooms, which require efficient speech transmission, it is effective to obtain a nonreverberant sound field by treating sound absorption in a minimum area on the walls that can provide the necessary and sufficient absorption. For such a reason, in this work, the acoustic effect of HSS treatment in relatively small rooms is investigated. As measures for the investigation, numerical methods such as the finite-element method (FEM), boundary-element method (BEM), and FDTD method based on the discrete numerical scheme of the sound wave equation are used [14,15]. Among them, as a useful measure for predicting the time-transient characteristics of sound fields in particular, the FDTD method was adopted in this study. The numerical method was initially proposed by Yee [16] in the field of electromagnetics, and it has been applied to room acoustic problems [13,17]. In this research, the sound absorption characteristics of HSS on the walls were evaluated by objective measure based on acoustical indices, including the reverberation time and clarity, which were obtained from the impulse responses calculated by the FDTD method. In addition, the subjective effect caused by HSS treatment was investigated through the subjective evaluation test based on the calculated impulse responses.

This paper is organized as follows. In Sect. 2, we describe the details of the investigated types of HSS, and those of the numerical and experimental studies. The numerical scheme for the sound field calculation by the FDTD method was firstly validated through comparison with the measurement results in Sect. 2.3. Then, the results obtained by the studies described in Sect. 2.1 and 2.2 are discussed in Sect. 2.4. In Sect. 3, the subjective effect of HSS on the reverberance of the evaluated rooms is discussed.

2. NUMERICAL AND EXPERIMENTAL STUDIES

2.1. Numerical Scheme

Figure 1 shows the investigated models of rooms (a), (b) and (c). The numerical study described in this section

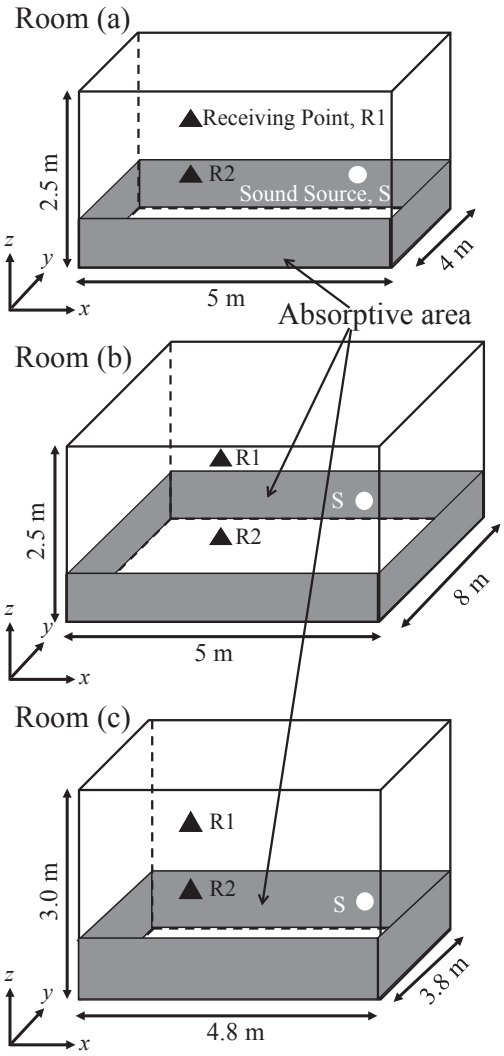

Fig. 1 Details of the simulated models of rooms (a), (b) and (c) with their dimensions and the source and receiving points.

was performed under the conditions of rooms (a) and (b), whereas the validity of the simulation (Sect. 2.2) was confirmed using room (c).

The dimensions of room (a) are 5 m (W) × 4 m (D) × 2.5 m (H), whereas those of room (b) are 5 m (W) × 8 m (D) × 2.5 m (H). The floor area of room (b) is twice as large as that of room (a). The acoustical effect of absorption treatment on the strip-shaped wall part indicated in gray in the figure is investigated. To investigate how the absorption efficiency varies when the arrangement of the absorbers is changed, the reverberation characteristics inside the rooms with the absorption conditions of A, B, C, D, E, F and G (Fig. 2) with fixed points of source S and receiver R1 and R2 are determined. Figure 2 shows only the setting condition of HSSs on one surface among the four surrounding walls in the room. Under each condition, HSSs having an equivalent total area of absorption (10.8 m^2) are shifted from the top to the bottom of the room, as shown in Fig. 2. Only under the split-type

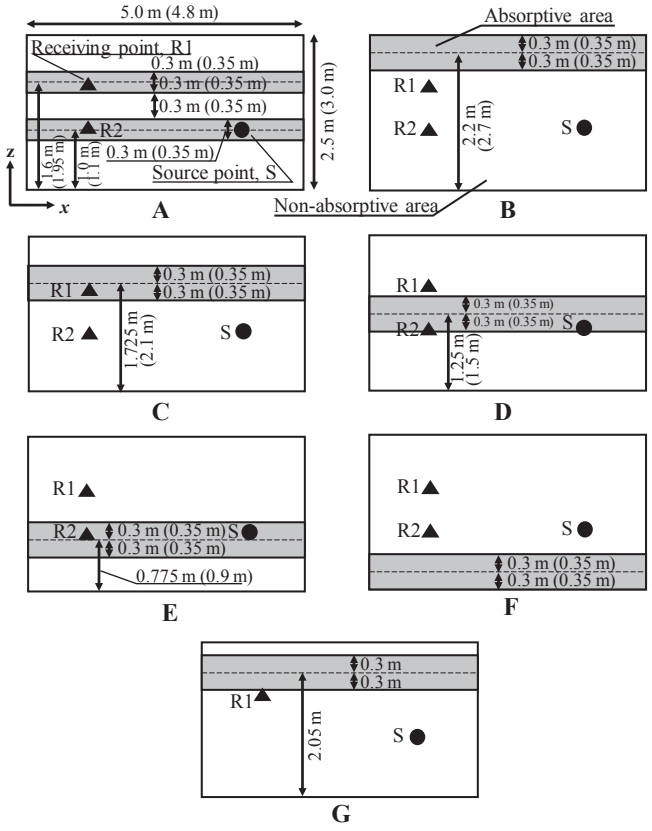

Fig. 2 Spatial relationship between receiving and source points, and the absorptive area. The dimensions enclosed by parentheses indicate those of room (c), whereas those without any parentheses indicate those of room (a) and (b).

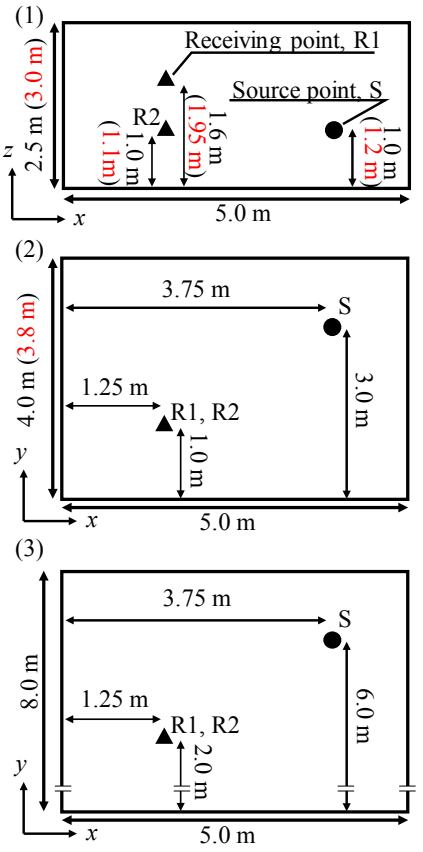

Fig. 3 Spatial relationship of the source and receiving points in the cross sections of the simulated rooms. (1) Cross section in the x–z plane of rooms (a), (b) and (c), in which the red values indicate the dimensions of room (c), (2) cross section in the x–y plane of rooms (a) and (c), in which the red values also indicate that of room (c), and (3) cross section in the x–y plane of room (b), respectively.

condition of A, the absorption area is divided into two parts so that each part of the absorption surrounds the source or receiving point. To investigate the effect of the spatial relationship among the source point, receiving point, and height of the surrounding HSS, the revised condition of G is set by moving up the absorbed area by 0.325 m from the position under condition C. Herein, the HSS of condition C spatially surrounds the source point, whereas the HSS of condition G does not. The spatial relationships between the source and receiving points in the case of rooms (a), (b), and (c) are shown in Figs. 3(1), 3(2), and 3(3). As shown in Fig. 3(1), the height of the receiving point of 1.6 m is set assuming that to be the head position of a standing adult, whereas the source point is set at 1.0 m, the head position of a sitting adult. Only under the condition of room (c), the heights of the receiving and source points are increased to 1.95 and 1.2 m, respectively, as indicated by the red values in the figure. The receiving and source points of rooms (a) and (c) are located in the plane shown in Fig. 3(2), whereas those of room (b) are located in the plane shown in Fig. 3(3).

The sound fields inside rooms (a) and (b) are calculated by the three-dimensional FDTD method. In the simulation,

Table 1 Frequency characteristics of the normal-incidence acoustic impedance on the absorptive surface.

Frequency [Hz]	125	250	500	1k	2k
Sound abs. coef. [—]	0.3	0.5	0.9	0.9	0.9
Acoust. Impedance [Pa·s/m^3]	4,600	2,390	788	788	788

the discrete spatial intervals and discrete time sampling are set as $\Delta x = \Delta y = \Delta z = 0.025$ m and 40,000 Hz, respectively. As the omnidirectional point source model, the Gaussian sound source is adopted. As the boundary condition of the absorptive surface, the real number acoustic impedances shown in Table 1, which are equivalent to the normal-incidence sound absorption coefficients in Fig. 4 simulating the typical characteristics of a glass fibrous material with a density of 25 kg/m^3 and a thickness of 50 mm, are given, whereas the acoustic impedance of the nonabsorptive surface is set to 15,500 Pa·s/m^3, which is equivalent to the normal-incidence sound absorption

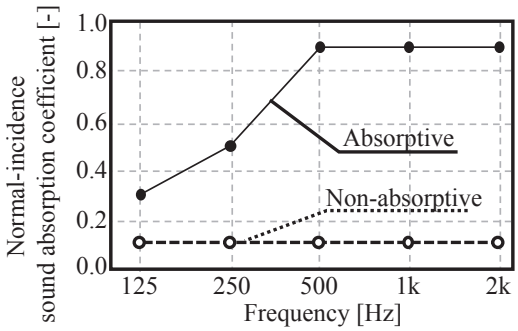

Fig. 4 Frequency characteristics of the normal-incidence sound absorption coefficient of the absorptive and nonabsorptive surfaces.

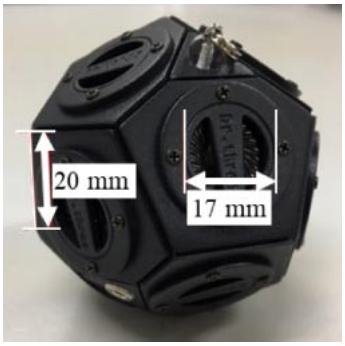

Fig. 5 Miniature dodecahedral speaker adopted in the scale model experiment.

coefficient of 0.1. To simulate the frequency characteristics shown in Table 1, the following calculation was performed. Firstly, the sound fields inside the rooms were calculated five times by changing the surface acoustic impedance into each value of 125, 250, 500, 1k, and 2k Hz shown in Table 1. Secondly, the transient responses in each frequency band among 125, 250, 500, 1k, and 2k Hz were filtered using the IIR filter. Herein, the data lengths of the adopted filters are sufficiently smaller than those of the transient responses under each condition. Lastly, the reverberation time and early decay time (EDT) in each frequency band were evaluated using the obtained transient responses. The reverberation time was calculated by integrated impulse response method over a 30 dB decay range in the reverberation curve from -5 to -35 dB below the starting level. The EDT was, on the other hand, calculated by the same method as that for the reverberation time over a 10 dB decay range in the reverberation curve from 0 to -10 dB below the starting level. In addition to these indices, to estimate the effect of the reverberation on sound clarity, the Clarity C_{80} and the Deutlichkeit D_{50} were also evaluated. However, the transient response of the calculated sound should be separated into two parts: the segments before and after the threshold time of 80 ms for the former and 50 ms for the latter, which are the durations between the arrival time of the direct sound and the time of the separation. Then, considering the ease of recognition of the exact incoming time of the direct sound, the transient responses were firstly separated into the two parts before the filtering treatment of the waveforms. After filtering for these two segments into 125, 250, 500, 1k, and 2k Hz components, the total sound energies of the former and latter segments in each octave band were calculated, and finally, C_{80} and D_{50} were obtained.

2.2. Experimental Scheme

To validate the numerical results obtained by FDTD analysis, a scale model experiment focusing on a rectangular room model with the dimensions of 0.96 m × 0.76 m × 0.6 m, which is the 1/5-scale model of room (c) shown in Fig. 1(c), was performed. The model is made with six sheets of 20-mm-thick acrylic plates. The sound source S and the receiver R1 were set as shown in Fig. 1(c), and the impulse response inside the sound field was measured by the swept-sine method. Then, to obtain impulse responses with the highest signal-to-noise ratio possible, the impulse response between S and R1 was measured using the linearly swept sine signal with the time duration of 2^{21} samples in 48 kHz sampling. The target frequency range of the impulse response measurement was set from 630 Hz to 10 kHz in the octave band frequency range, which corresponds to 125 Hz to 2 kHz. Note that the multiple synchronous averaging method was not carried out in this study, because the background sound level inside the acrylic box was relatively low so that impulse responses with a sufficient decay level of over 60 dB could be obtained. As a sound source that can be acoustically regarded as a point source in the frequency range from 630 Hz to 10 kHz, a miniature dodecahedral speaker with a side length of 20 mm, as shown in Fig. 5, was used in the measurement. This speaker includes twelve baffles of 17 mm diameter. The measurement results of the spatial directivity of the sound reproduction by this speaker in each octave band frequency are shown in Fig. 6. While the directivity of the sound has a slightly nonuniform distribution in a relatively high frequency range, the speaker generally has omnidirectional sound radiation characteristics. The absorption by HSS was treated as shown in Fig. 2 by pasting felt of 3.5 mm thickness on the surface inside the acrylic model. The random-incidence absorption coefficient of the felt measured by the reverberation room method is shown in Table 2. The random-incidence absorption coefficient was measured in a rectangular reverberation room of 1/10 scale with dimensions of 0.794 m × 0.630 m × 0.500 m. Then, the air in the model was replaced with nitrogen to avoid the air absorption of sound as much as possible. The dimensions of the width of

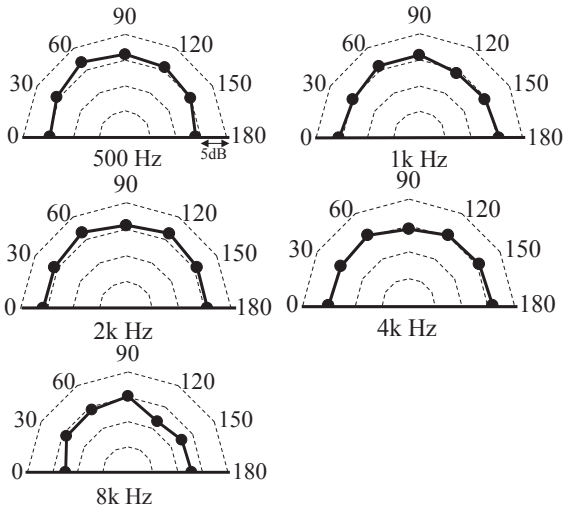

Fig. 6 Measurement results of the directivity of the sound reproduction by the adopted dodecahedral speaker in each octave band frequency.

Table 2 The absorption coefficients of the felt measured by the reverberation room method.

Frequency [Hz]	630	1.25k	2.5k	5k	10k
Rand. Abs. Coef. [—]	— (0.10)	0.20	0.47	0.88	1.02
Norm. Abs. Coef. [—]	0.06	0.13	0.34	0.81	0.90
Acoust. Impedance [Pa·s/m^3]	26,500	11,700	3,970	1,070	790

HSS in this validation study are enclosed by parentheses in Fig. 2.

The impulse response inside room (c) was also calculated by the FDTD method. The basic scheme of the calculation is the same as that described in Sect. 2.1, whereas the dimensions of the room and HSS are different from those shown in Sect. 2.1. The discrete spatial intervals and discrete time sampling are set the same as those mentioned in Sect. 2.1. As the boundary condition of the absorptive and nonabsorptive surfaces, the real number acoustic impedances shown in Tables 2 and 3 are equivalent to the normal-incidence sound absorption coefficients indicated in the same tables. Furthermore, the above-mentioned normal-incidence sound absorption was converted from the random-incidence sound absorption coefficient indicated in the same tables, on the basis of Paris' theory [18]. Herein, two points should be noted as follows. The first point is that the absorption coefficient of the felt in the 630 Hz band was assumed to be 0.1 in this study, because that could not be obtained by the reverberation room method owing to the limitation of the lower edge

Table 3 The absorption coefficient of the acrylic measured by the reverberation room method.

Frequency [Hz]	125	250	500	1k	2k
Abs. Coef. [—]	0.0012	0.0013	0.0017	0.0240	0.0490
Norm. Abs. Coef. [—]	0.007	0.008	0.011	0.015	0.031
Acoust. Impedance [Pa·s/m^3]	233,000	204,000	148,200	108,500	52,050

frequency of the measurement. The second point is that the random-incidence absorption coefficient of the surface of the acrylic was also estimated from the reverberation times measured inside the acrylic model.

2.3. Validation of Numerical Results

The validity of the numerical results obtained by the FDTD method is confirmed by comparing with the measured reverberation characteristics of the impulse responses. The results of reverberation time estimated from the numerical and experimental investigations are shown in Figs. 7(1) and 7(2), respectively. Under the 500 Hz octave band, almost all the results excluding the

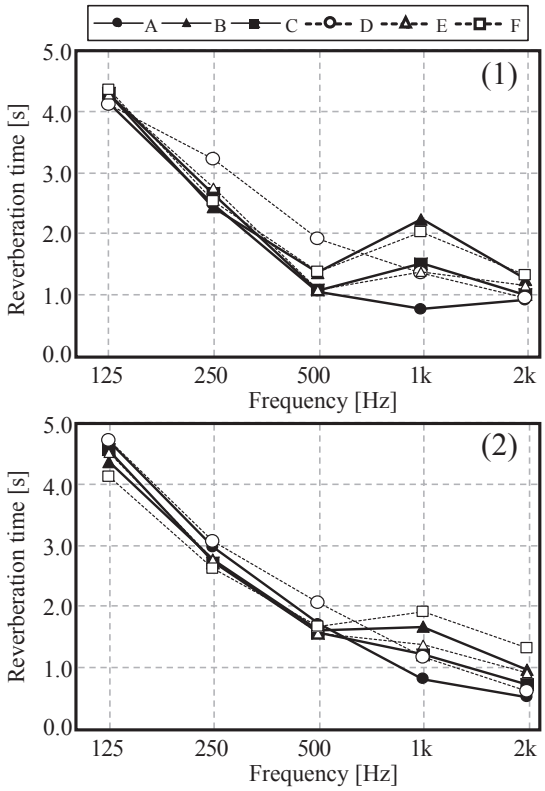

Fig. 7 Comparison between the (1) calculated and (2) measured reverberation times inside room (c).

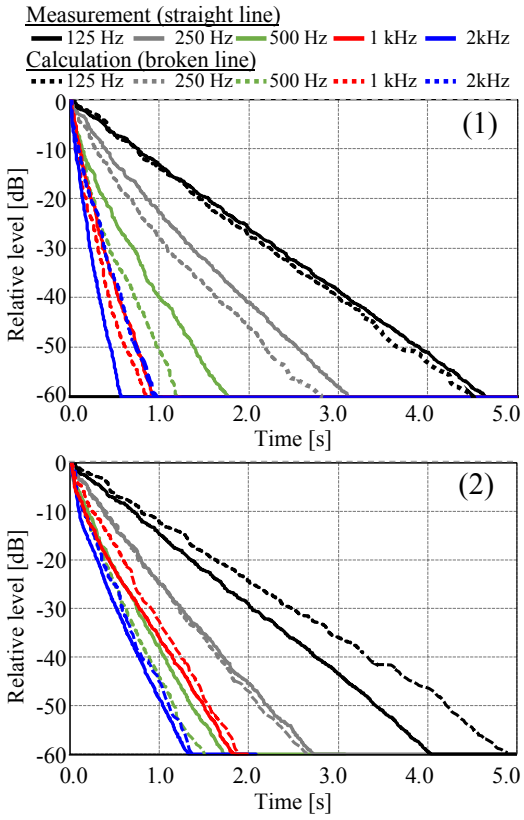

Fig. 8 Comparison of the Schroeder's decay curves obtained by the calculation and measurement. The results obtained for HSS conditions of (1) A, and (2) F, respectively.

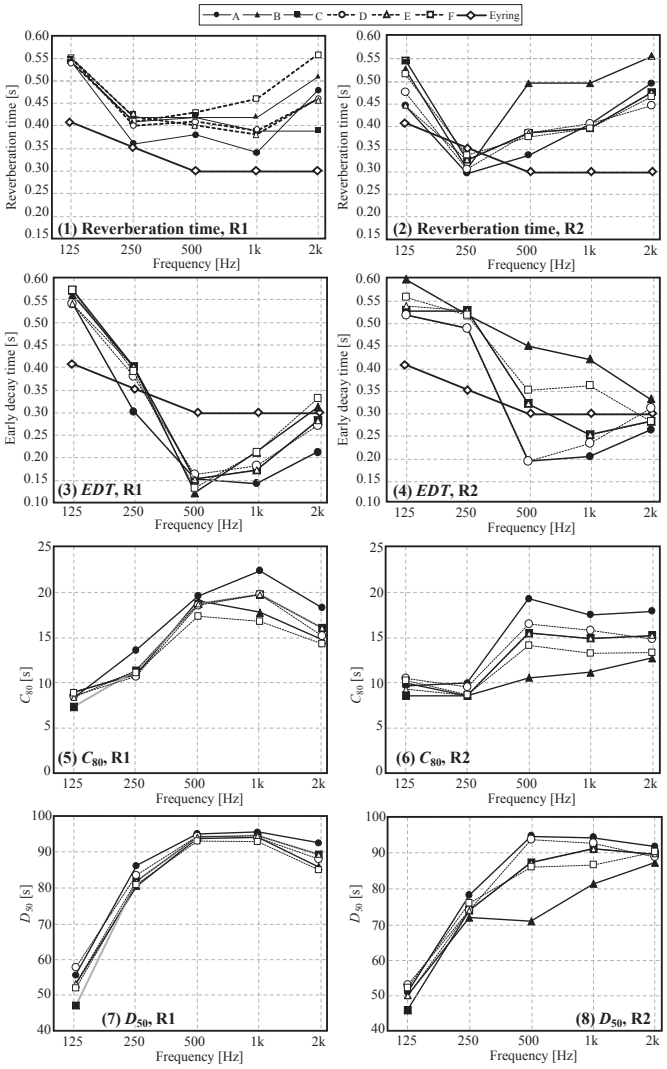

Fig. 9 Frequency characteristics of the simulated acoustic indices for the sound field inside room (a). (1), (3), (5), and (7) indicate the reverberation time, EDT, C_{80}, and D_{50} obtained at R1, whereas (2), (4), (6), and (8) indicate the reverberation time, EDT, C_{80}, and D_{50} obtained at R2.

condition of D indicate similar characteristics, whereas only those of D indicate slightly longer reverberation time. These tendencies are observed in both numerical and experimental results. On the other hand, the reverberation times of the 1 kHz octave band under each condition have been widely varied. In the numerical results of (1), the reverberation times of the HSS conditions of B and F are longer, whereas those of the other conditions are shorter. Among all the conditions, the condition of A indicates the shortest reverberation time in both the numerical and experimental results. On the other hand, Schroeder's decay curves of the rooms in the conditions of A and F are shown as examples in Figs. 8(1) and 8(2), respectively. The decay curves obtained from the numerical and experimental investigations for both settings of the HSS conditions of A and F are generally exponentially decayed, and they show relatively similar decay tendencies. As can be seen in these results, the numerical results were confirmed to agree reasonably well with the real room-acoustic phenomena inside a scaled model.

2.4. Results and Discussion

2.4.1. Effect of HSS on each of the room-acoustic indices

The frequency characteristics of the reverberation time, EDT, C_{80}, and D_{50} at the receivers of R1 and R2 of room (a) are shown in Fig. 9. In the figure, from (1) to (4), the theoretically calculated reverberation times based on Eyring's theory are also shown. As the frequency increases, the difference in the reverberation times between the absorption conditions increases. Firstly, in the comparison between the HSS condition A and the others in (1), the reverberation time of condition A is shorter than those of the others between 250 Hz and 1 kHz. Secondly, the reverberation times of the HSS conditions of B and F, in which the absorbers are set directly under the ceiling or over the floor, are much longer than those of the other conditions especially in the 1k and 2k Hz bands. Thirdly, the numerically calculated results in all the frequency ranges indicate larger values than the theoretical values.

Next, Fig. (2) shows that the reverberation time of the HSS condition F decreased but that of B increased compared with those shown in Fig. (1), owing to the difference in the height of the receiving point. The EDTs in Fig. (3) show that all the conditions indicate similar characteristics, whereas those of Fig. (4) show variant characteristics depending on the conditions. However, these results include the same tendencies with reverberation time, in which the HSS conditions of B and F indicate longer times, and the other conditions indicate shorter times among the octave band frequency ranges of 500, 1k, and 2k Hz. C_{80} and D_{50} indicated in the figure from (5) to (8) basically show the same tendencies as the reverberation time and EDT, in which the HSS conditions of B and F indicate lower values, and the others indicate higher values. In these indices, the HSS condition of A also indicates the highest values corresponding to the shorter reverberation time. Schroeder's decay curves at the receiver R1 of room (a) calculated from the numerically obtained impulse responses of the conditions A and F in each octave band are shown in Figs. 10(1) and 10(2), respectively. In the frequency range of 500 Hz, 1k Hz, and 2k Hz, the curves have slightly bending parts in the early time at around 0.05 s. By comparing between the conditions A and F, the reverberation of the former case decays slightly faster than that of the latter case in the late time after 0.2 s. The above-mentioned results on the acoustic indices of room (a) indicate that HSSs with different shapes, such as the single or split types, or different height of arrangement make the reverberation characteristics of the rooms significantly different from each other, whereas all the absorbers have the same total area of absorption. It should also be noted that the higher absorption effect in the split type of condition A could be caused by the area effect, which can become more prominent by splitting the absorbers into smaller pieces.

Next, the frequency characteristics of the reverberation time of room (b) are shown in Fig. 11. Firstly, the results in Fig. (1) show larger differences between each condition than those of room (a) in Fig. 9(1), especially in the frequency range over 500 Hz. Just the same as the characteristics of room (a), the reverberation time of condition A is shorter than those of the other conditions over 500 Hz. The tendency of the longer reverberation time of conditions B and F is also observed under this room condition. In addition, these numerically obtained values are larger than the theoretical values, as with the situation

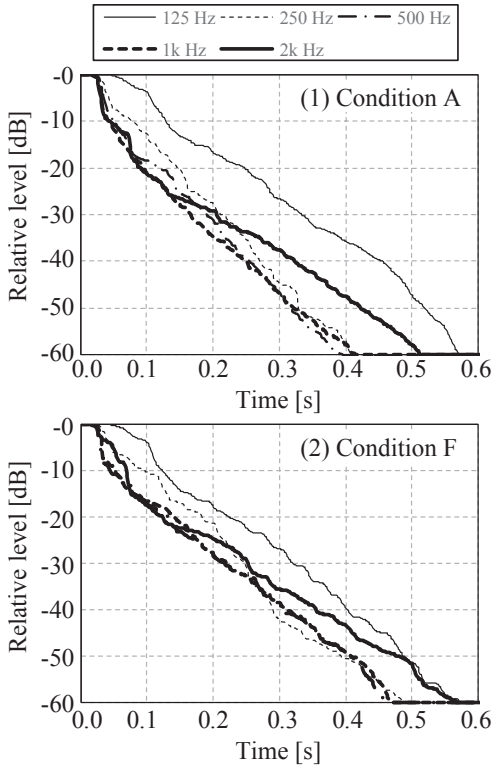

Fig. 10 Schroeder's decay curves of the calculated impulse responses at the receiver R1 of room (a) for HSS conditions of (1) A, and (2) F, respectively.

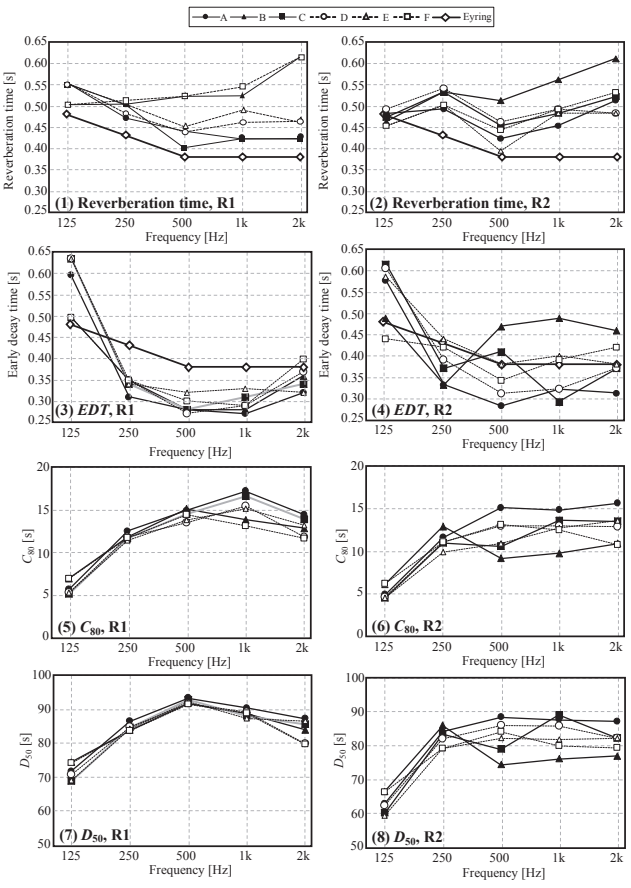

Fig. 11 Frequency characteristics of the simulated acoustic indices for the sound field inside the room (b). (1), (3), (5), and (7) indicate the reverberation time, EDT, C_{80}, and D_{50} obtained at R1, whereas (2), (4), (6), and (8) indicate the reverberation time, EDT, C_{80}, and D_{50} obtained at R2.

in the case of room (a). The EDT of Fig. (3) shows that all the conditions indicate similar characteristics, whereas that of Fig. (4) shows variant characteristics between each condition. These results also include the same tendencies as the reverberation time shown in Figs. (1) and (2). The C_{80} and D_{50} indicated in the figure from (5) to (8) basically show the same tendencies as the reverberation time and EDT, whereas the (5) C_{80} and (7) D_{50} under the condition of R1 show similar characteristics under all conditions.

On the basis of comparisons of these results of the room-acoustic indices in rooms (a) and (b), the following two points are discussed in relation to the abovementioned results.

The first point is that the variance between each HSS condition becomes larger, especially in the case of the reverberation times of both rooms (a) and (b) over 500 Hz. It has been reported in Ref. [13] that the reverberation times become longer especially in the middle frequency ranges owing to the low diffuseness of the sound field inside rooms, arising from the unevenly distributed absorbers. Because the absorbers are located in the corner of the room, especially under conditions B and F, it is considered that the nondiffuseness of the sound field under these conditions made the reverberation time much longer. The fact that the reverberation time is longer in the higher frequency range, even when the frequency characteristics of the absorption coefficients are flat [13], also supports the longer reverberation times, especially in the higher frequencies observed in (1) and (2) of Figs. 9 and 11. Note that, in this discussion, Ref. [13] referred to above, the effect of the absorbers set at the surface of the floors and ceilings was investigated, whereas in the present study, the HSS was set on the wall. In addition, the whole surface of the floors and/or ceilings was treated as absorbent in Ref. [13], whereas only some parts of the walls were treated as absorbent in this study. Although those studies started from different standpoints, they led to similar results that the partial absorption makes the sound diffuseness inside the room lower, and the reverberation characteristics inside the room are affected by the diffuseness.

The second point is that the deviation between each condition of the absorber is larger under the condition of R2 than under that of R1, especially in the results of the EDT, C_{80}, and D_{50}. In Ref. [13], it was reported that the reverberation time inside rectangular rooms can become longer in some cases, because the reverberation related to the two-dimensional mode frequencies excited in the horizontal plane inside the room enhances the reverberation of the room. In this case, the receiver R1 is located in the same plane as the source point S, whereas R2 is located in different plane. By considering these facts, the reverberation observed at R1 may include the dominant reverberation sounds excited in the two-dimensional mode of the horizontal plane including the point of R1 and the source, whereas R2 does not have such prominent modes as R1. It may be considered that such a dominant mode made the indices similar among each of the HSS conditions.

2.4.2. Effect of the height of arrangement of HSS on reverberation time

Figures 12(1) and 12(2) show the simulation results of the reverberation time at receiver R1 of rooms (a) and (b) rearranged in relation to the height of the arrangement of each absorber. Note that the HSS condition A is excluded from this figure, because only that condition has two types of height. Whereas the reverberation times shown in Fig. 12(1) in 125, 250, and 500 Hz have relatively flat characteristics regardless of the height of the absorber, those of 1 and 2k Hz have a downward projected shape with longer reverberation times under the conditions of B and F and shorter ones under the condition of C, D, E and G. Under the condition of room (b), not only the 2 kHz octave band frequency, but also 500 and 1k Hz octave band frequencies indicate the downward projected shape with shorter reverberation times under the conditions of C, D, and E. The results show that the difference in the height of HSSs has an appreciable effect on the reverberation time of narrow rooms in the higher frequency range. In the higher frequency range, especially 2 kHz, it is also observed that the reverberation times are shortened when HSSs are set at the same height as the receiving point. In addition, it is also

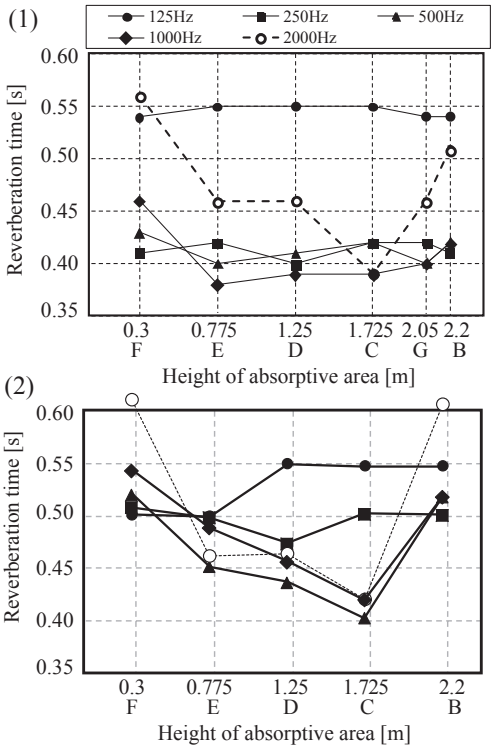

Fig. 12 Spatial distribution characteristics of the simulated reverberation times at the receiver R1 of the (1) room (a) and (2) room (b), respectively.

observed that the deviation of the reverberation times caused by the height of the location of the HSS is larger under the condition of room (b) than under that of room (a). The difference in the reverberation time is clearly seen in a wider frequency range including 500 Hz and 1 kHz, whereas those of the condition room (a) at 500 Hz and 1 kHz indicated relatively flat characteristics. Reference [13] also indicated that the frequency range, in which the reverberation time becomes longer owing to the unevenness of the absorber, decreases as the ceiling height increases. In this case, the same phenomena as above, in which the frequency range with the change in the reverberation time owing to the change in the location of the absorber widens to include the lower frequency range, are seen especially in the condition of room (b). Then, it may be considered that the effect of the location of the HSS can also be affected by the height of the room.

The above-mentioned results on the acoustic indices of both rooms (a) and (b) clarified that each of the HSS with different frequency characteristics has an effect on the absorption performance, which also varies depending on the size of the rooms and the location of the receiving points. However, in the case that the target room of absorption treatment has relatively large dimensions, such as the case of room (b) in this study, it was also confirmed that HSSs are effective when they are set on the surface of the walls at an appropriate height corresponding to the height of the receiving point.

3. SUBJECTIVE EVALUATION EXPERIMENT ON THE EFFECT OF HSS

In this section, the effect of HSS on the reverberation inside room (b) as shown in Fig. 1 is investigated through subjective evaluation experiments. Firstly, the impulse responses inside room (b) with HSSs on the walls are calculated by the FDTD method in the same manner as described in Sect. 2. Then, the subjectively perceived extent of the reverberation inside the room was investigated through subjective evaluation experiments using Scheffe's paired comparison method [19], and the results of the experiment were discussed with the acoustical characteristics of the room.

3.1. Details of the Subjective Evaluation Experiment

The difference in the subjective impression of reverberance caused by the presented stimuli was evaluated by Scheffe's paired comparison method, which was modified by Nakaya [19,20]. Nakaya's variation was adopted in this study, because the subjective evaluation for all the stimuli was performed by each of the subjects. In addition, by using that variation, the subjective effect of the order of the presentation of the paired stimuli need not to be considered in this study.

In this experiment, two types of stimulus, one is the impulse responses and the other is a male voice that includes the reverberation of the calculated rooms obtained as impulse responses in the former section, were presented to the subject via headphones (Audio-Technica, ATH-W1000Z). Here, the same monaural signals were simultaneously reproduced in the left and right channels of the headphone. The details of the generation scheme for these stimuli are described in the last part of this section.

Ten subjects consisting of five males and females between the ages of 20 and 60 participated. In total, 24 sets of stimuli, including two types of sound, two receivers, R1 and R2, inside room (b), and six types of HSS conditions, were adopted. Using Nakaya's variation of Scheffe's paired comparison method, the relative impression of one condition compared with the other one among each pair was evaluated on the relative scale shown in Fig. 13. The pairing scheme between each stimulus was designed as shown in Fig. 14. This pairing scheme considering limited pairs among each set of six stimuli, including the HSSs of A, B, C, D, E, and F, provides only the relationship of the relative impression of reverberation among different HSS

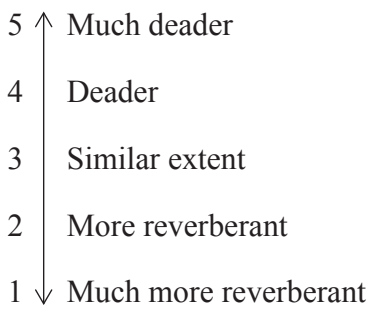

Fig. 13 Bipolar five categories adopted in the subjective evaluation experiment.

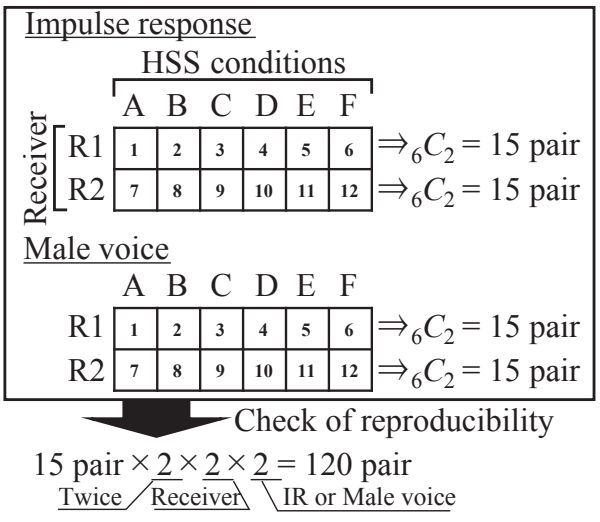

Fig. 14 Schematic of the pairing among each stimulus.

conditions. However, it takes a shorter time for the experiment because of the smaller number of pairing conditions. All the pairs were evaluated twice for each subject to check the reproducibility of their answers. Then, the 30 pairs for the six conditions from A to F including duplication for the check of reproducibility were resultantly evaluated four times in total. As a result, the total number of pairs for each subject was 120. The order of presentation of each stimulus was randomized in each set of evaluation of 30 pairs. The subjects were allowed to hear and compare the paired stimuli many times, because it is difficult to subjectively evaluate the difference in the reverberation with one trial.

To familiarize the subjects with the evaluation method, four randomly chosen conditions were additionally evaluated by the subjects as a trial, but the results of the trial evaluation were excluded from the analysis and discussion.

Next, the details of the method generating the two types of sound sources are described. While the calculated impulse response was directly reproduced as the first source, the sound obtained by convolution of the impulse response and a voice uttered by a Japanese male with the time duration of five seconds was adopted as the second source. The scheme of the signal processing to obtain the impulse response for auralization is as follows. Firstly, the calculated results in Sect. 2 are basically used for auralization. In Sect. 2.1, the calculated results, in which the surface acoustic impedance of HSSs was set to the values of each frequency band from 125 Hz to 2 kHz as shown in Table 1, were filtered using the IIR filter of 125, 250, 500, 1k and 2k Hz. After that, the filtered transient responses for each octave band of 125, 250, 500, 1k and 2k Hz were again overlapped. Resultantly, the impulse response including the desired frequency components from 125 Hz to 2 kHz octave bands can be obtained. Note that the auralized impulse response does not require any filtering by the inverse filter to correct the nonflat characteristics of the sound source given in the FDTD method, because that was performed by giving the flat characteristics of the frequency components from 88 to 2,828 Hz, which correspond to the lower edge frequency of the 125 Hz octave band and the upper edge frequency of the 2 kHz octave band, respectively.

3.2. Results and Discussion

Firstly, the reproducibility of evaluation by the 10 subjects was determined. Then, all the correlation coefficients between the evaluated scores of the repeated sets by all the subjects were greater than 0.8. For that reason, the responses given by all the subjects were considered in the statistical analyses of the results.

Secondly, the obtained evaluation results of receivers (1) R1 and (2) R2 in room (b) are shown in Figs. 15(1) and 15(2), respectively. In both results of (1) and (2), the difference in the score is more largely seen under the conditions of the impulse response than in those of the male voice, because the subjective difference in the reverberation can be more clearly perceived in the impulse response. The HSS conditions of B and F indicate lower scores, whereas that of A indicates a higher score. These tendencies correspond to those of the estimated results of the reverberation times in Fig. 11. Under the condition of receiver R1, the reverberation times of the HSS conditions of B and F over the 500 Hz octave band frequency are longer than the others, resulting in a similarly lower score in Fig. 11(1). Under the same condition of receiver R1, the reverberation times of the HSS conditions of A and C, especially in the 1 kHz octave band frequency, are shorter, resulting in similarly higher scores in Fig. 11(1). On the other hand, in Fig. 11(2), the reverberation time of the HSS under condition B is longer than that under F, and that under C is slightly longer than that under A. The scores shown in Fig. 15(2) also reflect the characteristic differences of the reverberation time.

As can be seen in the above-mentioned results of the subjective evaluation experiment, the differences in the reverberation characteristics caused by HSS, which were

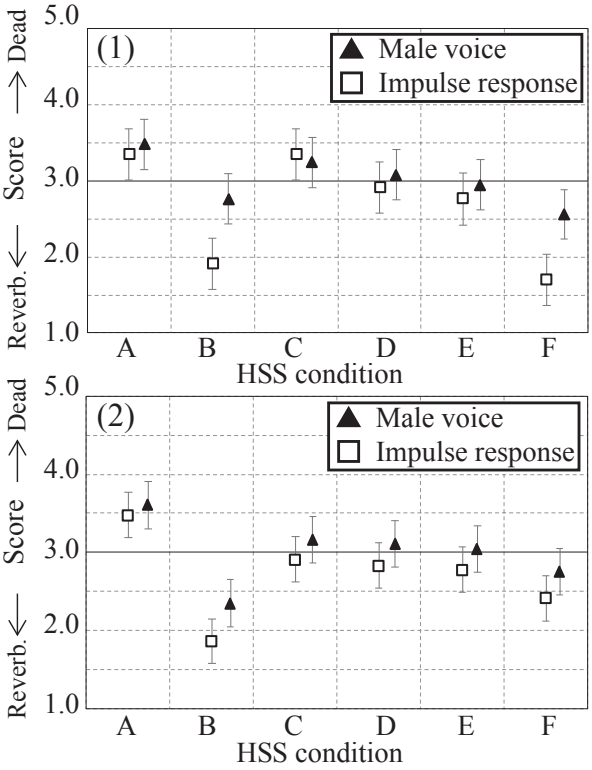

Fig. 15 The experimental results of the estimated relative scores in the conditions of the impulse responses obtained at (1) R1, and (2) R2, respectively. Herein, the error bars indicate the 95% confidence interval.

observed in the physical indices, were also confirmed from the viewpoint of the subjective impression.

4. CONCLUSIONS

The reverberation characteristics in rooms with HSS attached to the surrounding walls were investigated by three-dimensional FDTD analysis. The results of the case study confirmed that the frequency characteristics of the reverberation times of the rooms with HSSs were significantly varied under the influence of the relative positional relationship between the source and receiving points and the arrangement height of HSS. Through a subjective evaluation experiment based on Scheffe's paired comparison method, the differences in the effect of various HSS settings were also clearly observed as that of the subjective impression. On the basis of these results, it has been concluded that the HSSs arranged at several heights on the wall have different effects on the sound-absorption characteristics inside small rooms, whereas all the HSSs have identical surface areas. Some conditions of the height of the HSS indicated higher sound absorption, but their phenomena have not been completely elucidated. Thus, as a future work, further investigation of the mechanism of sound absorption by the HSS, especially the effect of the spatial relationship among the location and height of HSS, and the receiving and source points, should be carried out. Such detailed knowledge on the mechanism of the HSS can be conveniently applied to the practical design of the acoustics of small meeting rooms, which require a high speech transmission performance with suppressed reverberation.

REFERENCES

[1] A. M. Parvanian and M. Panjepour, "Mechanical behavior improvement of open-pore copper foams synthesized through space holder technique," *Mater. Des.*, **49**, 834–841 (2013).

[2] V. Chrisler, "Dependence of sound absorption upon the area and distribution of the absorbent material," *J. Res. Natl. Bur. Stand.*, **13**, 169–187 (1934).

[3] R. Cook, "Absorption of sound by patches of absorbent material," *J. Acoust. Soc. Am.*, **29**, 324–329 (1957).

[4] C. M. Harris, "The effect of position on the acoustical absorption by a patch of material in a room," *J. Acoust. Soc. Am.*, **17**, 242–244 (1946).

[5] A. Bruijn, "The sound absorption of an absorbing periodically uneven surfaces of rectangular profile," *Acustica*, **18**, 123–131 (1967).

[6] D. Takahashi, "Excess sound absorption due to periodically arranged absorptive materials," *J. Acoust. Soc. Am.*, **86**, 2215–2222 (1989).

[7] D. Guicking, "Theoretical evaluation of the edge effect of an absorbing strip of a pressure-release boundary," *Acustica*, **70**, 66–75 (1990).

[8] J. Ducourneau and V. Planeau, "The average absorption coefficient for enclosed spaces with non uniformly distributed absorption," *Appl. Acoust.*, **64**, 845–862 (2003).

[9] J.-B. Park, K. Grosh and Y.-H. Kim, "The effect of a periodic absorptive strip arrangement on an interior sound field in a room," *J. Acoust. Soc. Am.*, **117**, 763–770 (2005).

[10] K. S. Sum and J. Pan, "Characteristics of surface sound pressure and absorption of a finite impedance strip for a grazing incident plane wave," *J. Acoust. Soc. Am.*, **122**, 333–344 (2007).

[11] J. Wang, P. Leistner and X. Li, "Prediction of sound absorption of a periodic groove structure with rectangular profile," *Appl. Acoust.*, **73**, 960–968 (2012).

[12] D. Caballol and A. P. Raposo, "Acoustic absorption increase prediction by placing absorbent material in pieces," *Appl. Acoust.*, **113**, 185–192 (2016).

[13] Y. Yasuda, A. Ushiyama, S. Sakamoto and H. Tachibana, "Experimental and numerical studies on reverberation characteristics in a rectangular room with unevenly distributed absorbers," *Acoust. Sci. & Tech.*, **27**, 366–374 (2006).

[14] T. Okuzono, N. Shimizu and K. Sakagami, "Predicting absorption characteristics of single-leaf permeable membrane absorbers using finite element method in a time domain," *Appl. Acoust.*, **151**, 172–182 (2019).

[15] M. Toyoda, K. Funahashi, T. Okuzono and K. Sakagami, "Predicted absorption performance of cylindrical and rectangular permeable membrane space sound absorbers using the three-dimensional boundary element method," *Sustainability*, **11**(9), pp. 1–15 (2019).

[16] K. S. Yee, "Numerical solution of initial boundary value problems involving Maxwell's equations in isotropic media," *IEEE Trans. Antennas Propag.*, **AP-14**, 302–307 (1966).

[17] D. Botteldooren, "Finite-difference time-domain simulation of low-frequency room acoustic problems," *J. Acoust. Soc. Am.*, **98**, 3302–3308 (1995).

[18] E. T. Paris, "On the coefficient of sound-absorption measured by the reverberation method," *Philos. Mag.*, **5**, 489–497 (1928).

[19] H. Scheffe, "An analysis of variance for paired comparison," *J. Am. Stat. Assoc.*, **47**, 381–400 (1952).

[20] S. Nakaya, "Variation of Scheffe's paired comparison," *Proc. 11th Sens. Eval. Conv.*, pp. 1–12 (1970).